

# Functional Connectivity under Anticipation of Shock: Correlates of Trait Anxious Affect versus Induced Anxiety

Janine Bijsterbosch<sup>1,2</sup>, Stephen Smith<sup>1</sup>, and Sonia J. Bishop<sup>1,2</sup>

## Abstract

■ Sustained anxiety about potential future negative events is an important feature of anxiety disorders. In this study, we used a novel anticipation of shock paradigm to investigate individual differences in functional connectivity during prolonged threat of shock. We examined the correlates of between-participant differences in trait anxious affect and induced anxiety, where the latter reflects changes in self-reported anxiety resulting from the shock manipulation. Dissociable effects of trait anxious affect and induced anxiety were observed. Participants with high scores on a latent dimension of anxious affect showed less increase in ventromedial pFC–amygdala connectivity between periods of safety and shock anticipation. Meanwhile, lower levels of induced anxiety

were linked to greater augmentation of dorsolateral pFC–anterior insula connectivity during shock anticipation. These findings suggest that ventromedial pFC–amygdala and dorsolateral pFC–insula networks might both contribute to regulation of sustained fear responses, with their recruitment varying independently across participants. The former might reflect an evolutionarily old mechanism for reducing fear or anxiety, whereas the latter might reflect a complementary mechanism by which cognitive control can be implemented to diminish fear responses generated due to anticipation of aversive stimuli or events. These two circuits might provide complementary, alternate targets for exploration in future pharmacological and cognitive intervention studies. ■

## INTRODUCTION

Sustained fear responses—that is, prolonged physiological, subjective, and behavioral responses to a feared stimulus—are commonly experienced in the context of temporal unpredictability or uncertainty about the future occurrence of an aversive event (Grupe & Nitschke, 2013; Davis, Walker, Miles, & Grillon, 2010; Grillon, 2002). Why is it that some people cope relatively well with uncertainty regarding potential future adverse events, whereas others struggle with sustained fear? This question is of particular relevance to understanding anxiety disorders such as generalized anxiety disorder, where the pervasive experience of sustained anticipatory anxiety is a central feature.

Heightened sustained fear responses might arise as a result of excessive “bottom–up” responsivity to information indicating potential future threat, leading to amplification of the fear responses generated. However, failure to engage “top–down” mechanisms to regulate and diminish these fear responses might also play a role in their duration (Bishop, 2007). In other words, both exaggerated generation and impoverished regulation of fear responses could conceivably contribute to the pathological sustained fear responses observed in anxiety. To investigate this, we used a prolonged anticipatory anxiety paradigm to explore

whether individuals at elevated trait risk of developing anxiety disorders show altered function of brain circuits previously implicated in the generation and regulation of sustained fear.

Both basic, and more recently human, neuroscience studies have used fear conditioning paradigms to investigate the neural correlates of phasic and sustained acquired fear responses (Milad & Quirk, 2012; Davis et al., 2010; Delgado, Olsson, & Phelps, 2006; Sotres-Bayon, Bush, & LeDoux, 2004). Rodent fear conditioning experiments have highlighted the importance of the amygdala in acquisition and expression of conditioned fear (Kochli, Thompson, Fricke, Postle, & Quinn, 2015; Onishi & Xavier, 2010; LeDoux, 2003; Goosens, 2001), with the bed nucleus of the stria terminalis (BNST) being additionally implicated in expression of sustained fear (Davis et al., 2010). These findings are complemented by studies of unlearned fear responses in macaques, where amygdala lesions reduce fear responses across the board (Kalin, 2004) and heightened amygdala metabolism is linked to trait-like differences in anxiety (Fox, Shelton, Oakes, Davidson, & Kalin, 2008). Meanwhile, there is general consensus as to the centrality of the infralimbic ventromedial pFC (VMPFC) to fear extinction and extinction recall (Sierra-Mercado, Padilla-Coreano, & Quirk, 2011; Milad & Quirk, 2002) and of the hippocampus to the contextual modulation of fear learning (Maren,

<sup>1</sup>University of Oxford, <sup>2</sup>University of California, Berkeley

Phan, & Liberzon, 2013; Sotres-Bayon, Sierra-Mercado, Paredilla-Delgado, & Quirk, 2012). Many of these findings—especially as regards phasic fear—have been substantiated in humans using fMRI (Maren et al., 2013; Milad & Quirk, 2012; Delgado et al., 2006).

One of the main experimental procedures used to study the neural substrate of anticipatory anxiety in humans is a cued anticipatory anxiety paradigm (Grupe, Oathes, & Nitschke, 2013; Nitschke, Sarinopoulos, Mackiewicz, Schaefer, & Davidson, 2006). This involves presentation of a discrete cue stimulus, followed by an anticipation period, typically of 2- to 8-sec duration, after which an outcome stimulus is presented—for example, a negative picture or a burst of electrical stimulation. Other studies have used manipulation of the probability or temporal uncertainty of the occurrence of aversive stimuli to investigate anticipatory anxiety over longer periods (Somerville et al., 2013; Kalisch et al., 2005). Together, these studies have reported activation of a number of discrete regions during anticipation of threat, notably the extended amygdala (including the BNST), anterior insula, dorsolateral pFC (DLPFC), anterior midcingulate cortex (aMCC; as defined by Shackman et al., 2011), and VMPFC (Somerville et al., 2013; Nitschke et al., 2006; Simmons, Strigo, Matthews, Paulus, & Stein, 2006; Ploghaus et al., 1999). It has been proposed that activity in certain regions, such as the extended amygdala, aMCC, and anterior insula, may be linked to the generation and experience of anticipatory anxiety, as well as associated processes such as vigilance for threat (Straube, Mentzel, & Miltner, 2007; Kalisch et al., 2005). In line with this, activation of these regions during anticipation of aversive stimuli has been reported to be elevated in clinically and trait anxious individuals (Carlson, Greenberg, Rubin, & Mujica-Parodi, 2011; Nitschke et al., 2009; Straube et al., 2007; Simmons et al., 2006) and, in the case of the amygdala and anterior insula, to vary positively as a function of trial to trial self-reported anxiety (Carlson et al., 2011). In contrast, it has been suggested that activity in prefrontal regions such as DLPFC and VMPFC may support attempts at regulation of anxiety responses. Evidence for this comes from findings that deliberate regulation is associated with increased activation of lateral frontal regions during anticipation of potential pain (Kalisch et al., 2005), similar regions also being activated when reappraisal strategies are engaged to reduce emotional responses to other negative stimuli (Buhle et al., 2014), and from findings that sustained recruitment of VMPFC during anticipation of temporally unpredictable negative stimuli is associated with a reduced phasic amygdala response to such stimuli (Somerville et al., 2013). Converging evidence also comes from neuropsychological studies, where patients with VMPFC lesions have been found to show amygdala hyper-responsivity to negative stimuli (Motzkin, Philippi, Wolf, Baskaya, & Koenigs, 2015).

Functional connectivity analyses allow us to go beyond consideration of single brain regions and investigate the

coactivation of regions that together comprise circuits implicated in the expression or regulation of sustained fear responses. To date, investigations of the brain circuitry underlying pathological sustained anxiety responses, as indexed by functional connectivity, have primarily focused on connections that may underlie exaggerated generation and prolonged experience of sustained fear responses. Using 60-sec task blocks containing occasional shock delivery, McMenamin and colleagues reported an initial increase in within- and between-network insula connectivity followed by an increase in connectivity between the amygdala and other brain regions (McMenamin, Langeslag, Sirbu, Padmala, & Pessoa, 2014). High anxious individuals showed increased connectivity between the BNST and other brain regions during the shock scans (McMenamin et al., 2014). Using a prolonged (6 min) anticipation of shock manipulation uncontaminated by actual shock delivery, Vytal and colleagues reported that participants showed increased connectivity between amygdala, dorsomedial pFC, and insula under threat of shock, with heightened trait anxiety being positively associated with the extent of increased functional connectivity between amygdala and dorsomedial pFC (Vytal, Overstreet, Charney, Robinson, & Grillon, 2014).

The aim of the current study was to complement these prior investigations by examining whether individuals at elevated trait risk of anxiety show evidence of disrupted recruitment of circuitry subserving fear regulation during conditions likely to provoke sustained fear responses. It has been proposed that regulation of negative emotions including fear can be either automatic or deliberate (Mauss, Bunge, & Gross, 2007). A phylogenetically early connection between the VMPFC and the amygdala is held to subserve spontaneous down-regulation, whereas the DLPFC has been suggested to support engagement of voluntary regulatory strategies including cognitive reappraisal (Hartley & Phelps, 2010; though see Buhle et al., 2014). Findings that trait disposition to reappraise is linked to decreased anterior insula activity during anticipation of aversive stimuli (Carlson & Mujica-Parodi, 2010) raise the possibility that DLPFC–anterior insula connectivity might be of especial interest when considering circuitry that could facilitate regulation of anticipatory anxiety in humans, in addition to evolutionarily conserved VMPFC–amygdala mechanisms.

To investigate between-participant differences in DLPFC and VMPFC connectivity with the amygdala and anterior insula under conditions likely to promote sustained fear responses, we used a novel prolonged threat of shock paradigm that combines the actual administration of shock to increase anticipation (as in McMenamin et al., 2014) with examination of functional connectivity during a long period of shock anticipation free from shock administration (as in Vytal et al., 2014; but with this period extended to 15 min). We adopted a regularized

partial correlation approach (Marrelec et al., 2006) to examine functional connectivity between our four ROIs: DLPFC, VMPFC, amygdala, and anterior insula.

We tested the following two hypotheses. First, in line with models of automatic emotion regulation and its potential role in successful fear down-regulation (Hartley & Phelps, 2010; Mauss et al., 2007), as well as prior accounts indicating altered VMPFC–amygdala structural and functional connectivity in anxiety (Kim, Gee, Loucks, Davis, & Whalen, 2011; Kim & Whalen, 2009), we predicted that individuals high in anxious affect would show impoverished augmentation of VMPFC–amygdala connectivity during sustained anticipation of threat. Second, we predicted that increased DLPFC connectivity with regions implicated in the experience of anticipatory anxiety, in particular the anterior insula, would be linked to lower levels of self-reported induced anxiety (anxiety linked to the threat of shock manipulation). This second prediction follows from the proposed role of DLPFC in the deliberate cognitive regulation of fear responses, together with findings indicating that trait reappraisal is linked to decreased anterior insula activity during anticipation of threat and that activation of this latter region covaries with self-reported anticipatory anxiety (Carlson et al., 2011; Carlson & Mujica-Parodi, 2010; Hartley & Phelps, 2010). Finally, we were interested in whether individual differences in recruitment of this DLPFC circuitry under threat of shock would be independent of trait anxiety or whether engagement of this circuitry would be impoverished in high trait anxious individuals. If the former holds, then this could potentially reflect a mechanism through which individuals high in trait anxious affect might be able to compensate for dysregulation of VMPFC–amygdala circuitry.

## METHODS

### Participants

Thirty-two participants (14 men, all right-handed, aged 18–40 years, mean age = 24.8 years) took part. The study was approved by the Central University research ethics committee in Oxford and carried out in compliance with their guidelines. Written informed consent was obtained from participants before participation. Individuals with a history of psychiatric care, neurological disease or head injury, or taking psychotropic medication were excluded.

### Questionnaire Measures of Negative Affect

Participants completed eight standardized measures of negative affect in a separate screening session before the fMRI session. Individuals were prescreened to ensure that participants were included who scored toward the top, middle, and bottom of the range on self-report measures of anxious affect. Trait anxiety was measured

using the Spielberger State-Trait Anxiety Inventory (STAI form Y; Spielberger, 1983), which was broken down into two subscales (trait anxiety and trait depression) based on previous work (Bieling, Antony, & Swinson, 1998). The Mood and Anxiety Symptoms Questionnaire, which includes subscales for anxious arousal and anhedonic depression (Watson et al., 1995; Watson & Clark, 1991), was also administered. To obtain a measure of cognitive aspects of anxiety (i.e., worry), we included the Penn State Worry Questionnaire (Meyer, Miller, Metzger, & Borkovec, 1990). With regard to measures of depression, we included the Beck Depression Inventory (Beck, Ward, Mendelson, Mock, & Erbaugh, 1961) and the Center for Epidemiologic Studies Depression Scale (Radloff, 1977). These are the two most commonly used measures of depressive affect and provide coverage of the negative mood aspects of depression. From the personality literature, we administered the 80-item Eysenck Personality Questionnaire (EPQ; Eysenck & Eysenck, 1975). As the focus of this study is on anxious affect, we only used the Neuroticism subscale from the EPQ in our analyses. Principle component factor analysis with Varimax rotation was applied to the eight questionnaire measures of negative affect, leading to the identification of two latent dimensions of affective style: one primarily indexing trait anxious affect and one primarily depression-related affect. The former is used as the measure of trait anxious affect throughout the study reported here. The benefit of this approach is that noise related to idiosyncratic aspects of each self-report measure can be eliminated. Participants also completed the STAI state subscale immediately before entering the scanner.

### fMRI Acquisition

Two runs of fMRI data were acquired using a Siemens Verio 3T MRI system (Berlin, Germany) with 32-channel head coil. For the “safe” scan, participants were instructed to lie still, keep their eyes open, and stay awake. For the “shock” scan, participants were given identical instructions, but were told that they would receive randomly timed electric shock stimuli throughout the scan (“*sometimes close together and sometimes with long gaps between stimuli*”). A fixation cross was shown on the screen during both scans. A multiband EPI sequence was used (acceleration factor = 6, repetition time [TR] = 1140 msec, echo time = 40 msec, flip angle = 66°, 66 slices, 2 × 2 × 2 mm voxel size covering the whole brain; Feinberg et al., 2010; Moeller et al., 2010). The “safe” scan lasted for 15 min (790 volumes). This was followed by the “shock” scan, which comprised three parts: an initial 5-min period (268 volumes) during which shocks were actually received at intermittent intervals, a subsequent 15-min period (790 scans) during which no shocks were received, and a final 2-min period (100 scans) during which shocks were received. These three stages were conducted within a single fMRI scan (1158 volumes), and participants were

not given any information regarding this three-part structure but were simply told to expect shocks at unpredictable intervals throughout and that there could be long gaps between shock stimuli. A number of relatively long intervals were included between shocks in the first part of the scan to maintain participants' expectancy of shock throughout the following "anticipatory" period.

Before the two functional runs, structural images were acquired using a T1-weighted 3-D MPRAGE sequence with whole-brain coverage (TR = 2040 msec, echo time = 4.7 msec, flip angle = 8°, slice thickness = 1 mm). B0 fieldmaps were acquired after the "shock" scan to correct for distortions resulting from B0 inhomogeneity (Ugurbil et al., 2013; Cusack, Brett, & Osswald, 2003; Jezzard & Balaban, 1995).

### Electrical Shock Stimulation and Experimental Design

Electric stimulation was administered using a DS7A constant current stimulator (Digitimer, Hertfordshire, UK) and consisted of individual 2-msec square-wave pulses delivered to the inside of the forearm via a surface electrode with platinum pin (WASP electrode, Specialty Developments, Kent, UK). Low pass filters (BLP-1.9+, 50 OHM, DC-1.9 MHz, Mini-Circuits, Brooklyn, NY) were used at the interface with the Faraday cage. The intensity of the electric stimuli was calibrated for each participant after the "safe" scan and before the "shock" scan using an incremental step procedure. Stimulation intensity was increased in small steps, and participants were asked to identify the stimulus intensity that would be equivalent to a subjective rating of 7 on a numerical scale ranging from 0 (*no pain*) to 10 (*worst pain imaginable*). The shock intensity that participants equated to a subjective level of 7 ranged from 0.81 to 47 mA (mean = 3.89 mA, median = 2.21 mA). There was one outlier, the participant who chose a shock intensity of 47 mA. Excluding this outlier participant, shock intensity ranged from 0.81 to 6.81 mA with a mean of 2.46 mA and a median of 2.11 mA. This outlier participant was not an outlier on any questionnaire measures or connectivity indices and was therefore included in all further analyses. The removal of this participant did not change any of the results reported here.

Participants were instructed that randomly timed stimuli would be experienced throughout the "shock" scan. In fact, shock stimuli only occurred in the first 5 min and last 2 min of the experiment. This design allowed us to acquire 15 min of fMRI data under heightened anticipation of aversive stimuli, but with no stimulation confounds. A total of 15 stimuli occurred in the first 5 min (separated by 0.5–150 sec, mean = 21 sec, median = 2 sec), and five stimuli occurred in the last 2 min (separated by 0.5–100 sec, mean = 27 sec, median = 3 sec). The timing of the stimuli was pseudorandomized and kept constant across participants.

### Measurement of Induced Anxiety

To assess the effect of the shock manipulation on levels of induced anxiety, participants responded to the question: "How anxious did you feel during the last scan?" immediately after both the "safe" and "shock" scans. Participants answered using a button box to identify their response on a visual analogue scale ranging from 1 (*not at all*) to 7 (*very much*). "Induced Anxiety" was calculated as the zero-meaned difference in self-reported anxiety following the shock scan versus following the safe scan.

### fMRI Preprocessing

Preprocessing was conducted using FSL (FMRIB Software Library, Version 6.00, www.fmrib.ox.ac.uk/fsl), and followed the standardized preprocessing pipeline from the Human Connectome Project (Glasser et al., 2013; Smith et al., 2013). Motion correction was conducted using FMRIB's linear image registration tool MCFLIRT (Jenkinson, Bannister, Brady, & Smith, 2002; Jenkinson & Smith, 2001). Nonsaturated EPI images were used as registration reference images, as they have higher tissue contrast than the (saturated) EPI time series data. B0 unwarping was performed in FUGUE (FMRIB's utility for geometrically unwarping EPIs) using acquired fieldmaps (Ugurbil et al., 2013; Cusack et al., 2003; Jezzard & Balaban, 1995). Minimal high-pass temporal filtering (cutoff full-width 2000 sec) was performed to remove low-frequency drift, and no spatial smoothing was applied (Smith et al., 2013). EPI data were registered to the individual's skull-stripped structural image (Smith, 2002), using linear affine boundary-based registration (Greve & Fischl, 2009; Jenkinson et al., 2002; Jenkinson & Smith, 2001). Structural to standard space registration was conducted using linear registration (FLIRT, 12 degrees of freedom) and refined using nonlinear registration (FNIRT; Andersson, Jenkinson, & Smith, 2007a, 2007b).

To minimize influences of scanner-related and physiological noise, single-subject ICA was performed using FSL's MELODIC (Beckmann & Smith, 2004). Artifactual components were labeled using FMRIB's ICA-based X-noisefier (FIX; Griffanti et al., 2014; Salimi-Khorshidi et al., 2014), and all FIX component labels were manually checked. Unique variance associated with artifactual ICA components and motion confounds (24 regressors: six motion parameters, six first derivatives, and the squares of these 12 regressors) was removed from the data.

Following preprocessing, the "shock" scan was split into three parts: the initial 5 min (268 volumes) containing electric shock stimuli ("initial shock"), the 15 min (790 volume) "shock anticipation" period, and the final 2 min (100 volumes) containing shock stimuli ("end shock"). The 15-min "safe" and "shock anticipation" scans were used in all analyses described below unless otherwise stated.

## ROIs

Our four ROIs—the amygdala, anterior insula, VMPFC, and DLPFC—were taken from a more extensive set of ROIs implicated in emotional processing and regulation (Bijsterbosch, Smith, Forster, John, & Bishop, 2013). VMPFC and amygdala ROIs were defined using the Harvard–Oxford template (thresholded at 50% probability), DLPFC was defined functionally using an attentional task data, and the anterior insula ROI was defined using functional task data to split the Harvard–Oxford Insula ROI into anterior versus posterior subdivisions (see Bijsterbosch et al., 2013).

Principal eigen time series were extracted from these four ROIs for each participant and for each scan. Time series from bilateral regions were extracted separately for the left and right regions and subsequently averaged before the calculation of connectivity matrices. This is important when conducting partial correlation analyses as bilateral regions are commonly very highly correlated, and their separate inclusion in such analyses leads to unacceptable degrees of colinearity.

## Calculation of Connectivity Matrices

Partial correlation with Tikhonov regularization (0.1), as provided by FSLnets (fsl.fmrib.ox.ac.uk/fsl/fslwiki/FSLNets), was used to calculate  $4 \times 4$  connectivity matrices for each participant and for each scan. By conditioning the dependencies between two brain regions on all other brain areas included in the matrix, partial correlation aims to provide a better measure of “direct” functional connectivity than does full correlation (Marrelec et al., 2006).

Time-averaged connectivity matrices were calculated using all 790 time points from the “safe” scan and from the “shock anticipation” period of the second scan. These were in turn used to calculate difference connectivity matrices (“anticipation of shock” minus “safe”) for each participant. We also calculated partial correlation matrices from nonoverlapping time windows across the “safe” scan and both the “initial shock” and “shock anticipation” periods of the second scan (window length = 150 sec = 131 TRs, 14 windows in total). A linear regression line was fit to the data from the last six windows (the “shock anticipation” period). This enabled investigation of whether any changes in connectivity in response to our shock manipulation developed or waned across this period. All partial correlation matrices were converted to  $z$  scores before further analyses.

## Regressing Differences in Connectivity onto Trait Anxious Affect and Induced Anxiety

Participant-level indices of change in connectivity (“anticipation of shock” minus “safe”) were entered as dependent variables in a general linear model regression

analysis, with either individual differences in trait anxious affect or induced anxiety being entered as the between-participant predictor variable. An additional analysis was also conducted with both anxious affect scores and induced anxiety scores entered together to determine the independent effects of these variables.

## Replication of Amygdala–aMCC Results

We did not have aMCC as an initial a priori ROI. However, with the publication of the work by Vytal et al. (2014) and given the value of replication, we conducted additional analyses using an aMCC ROI taken from our prior work (Bijsterbosch et al., 2013). This region maps onto the dorsomedial pFC ROI used by Vytal and colleagues and has elsewhere been reported to show increased activity during anticipation of threat (Grupe et al., 2013; Kim et al., 2011; Straube et al., 2007; Nitschke et al., 2006). This ROI is defined based on the Harvard–Oxford ROI (50% probability threshold) for the ACC between  $y = 4.5$  and  $y = 30$  (Shackman et al., 2011). It was added as a fifth region, and partial correlation matrices during “safe,” “initial shock,” and “shock anticipation” periods were recalculated.

## RESULTS

### Factor Analysis of Questionnaire Measures

Principle component factor analysis performed on the eight measures of negative affect yielded two factors with eigenvalues greater than one (total cumulative explained variance 70.45%). The rotated component matrix is shown in Table 1 and reveals that the first factor (component explains 38.22% variance) primarily indexes anxious affect whereas the second factor (component explains 32.23% variance) relates mainly to depressed affect. Given

**Table 1.** Factor Analysis of Questionnaire Scores

	<i>Component</i>	
	<i>1</i>	<i>2</i>
STAI trait anxiety	0.805	–
STAI trait depression	0.788	–
EPQ Neuroticism	0.715	0.481
BDI	–	0.939
CESD	–	0.904
PSWQ	0.798	–
MASQ anxious arousal	0.412	–
MASQ anhedonic depression	0.607	0.645

This revealed latent dimensions of anxious and depressed affect. Component 1 shows particularly high loadings on the STAI and PSWQ, and Component 2 loads especially strongly on BDI and CESD. BDI = Beck Depression Inventory; CESD = Center for Epidemiologic Studies Depression Scale; MASQ = Mood and Anxiety Symptoms Questionnaire; PSWQ = Penn State Worry Questionnaire.

our focus upon anxiety, the first factor was used to investigate trait-level individual differences in functional connectivity under anticipation of shock.

### Analysis of Induced Anxiety as a Result of the Shock Manipulation

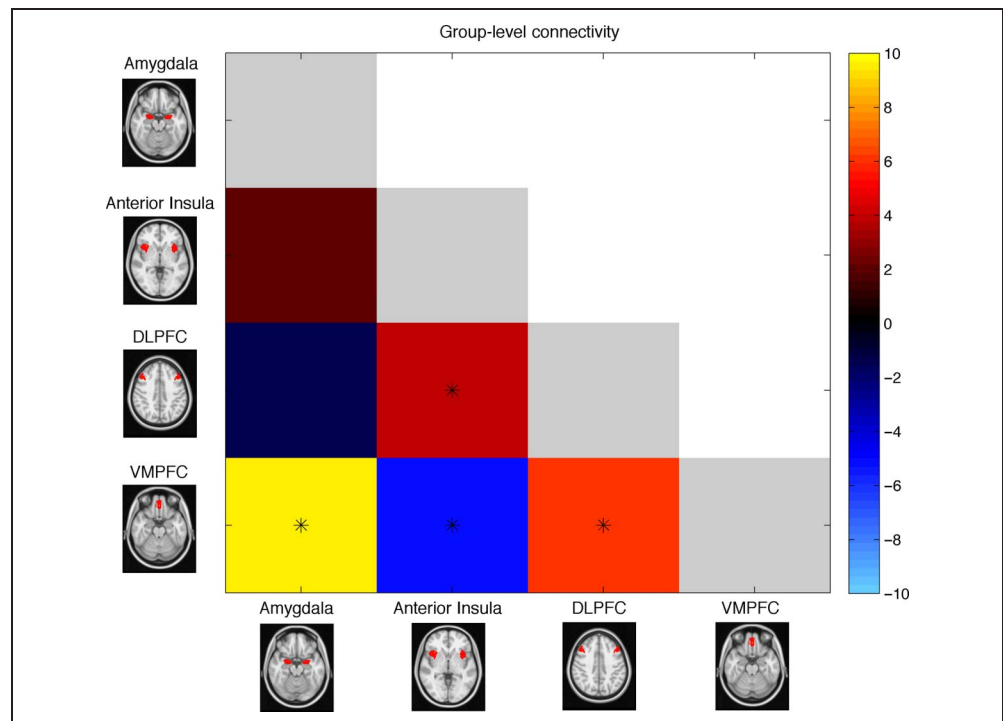
To assess the extent to which the shock manipulation induced anxiety, we compared responses to the question “How anxious did you feel during the last scan?” obtained inside the scanner immediately after each functional scan. A visual analogue scale with 7 points was used. A paired *t* test revealed that responses to this item were significantly higher after the “shock” than after the “safe” scan ( $t = 2.84, p = .008$ ). This result confirms that the shock manipulation successfully induced an elevation in anxiety levels (mean =  $2 \pm 1.1$  after “safe” scan and  $3 \pm 1.8$  after “shock” scan). The difference score (response after “shock” scan minus response after “safe” scan) obtained from this question was used to investigate differences in functional connectivity under anticipation of shock as a function of induced anxiety. This induced anxiety score was weakly correlated with STAI trait anxiety and with scores on the latent dimension of anxious affect ( $r = .34, p = .06$  and  $r = .28, p = .12$  respectively). There was no significant relationship between STAI trait anxiety or scores on the latent dimension of anxious affect and self-reported (analogue scale) anxiety for either the “safe” or “shock” scans when these were considered independently,  $p_s > .2$ . As is typically the case, current or “state” anxiety as measured by the STAI at the beginning of the experimental session was highly

correlated with STAI trait anxiety,  $r = .63, p < .001$ . In contrast, there was a nonsignificant correlation between STAI state anxiety and our measure of induced anxiety provoked by the shock manipulation  $r = .30, p = .10$ . This finding suggests that this induced anxiety score provides a sensitive measure of the manipulation of anxiety through the shock procedure that is only weakly related to general “current” or state anxiety as measured at the beginning of the experimental session. Neither induced anxiety scores nor scores on the latent dimension of anxious affect were correlated with shock intensity ( $|r| < 0.16, p > .4$ ).

### Group-averaged Connectivity Matrix

The mean of the two connectivity matrices estimated for “safe” and “shock anticipation” periods was calculated for each participant. A two-tailed one-group *t* test was performed using the resulting mean connectivity matrix for each participant to determine group-level connectivity between the four ROIs. Results are summarized in Figure 1 and reveal direct positive connectivity between the amygdala and VMPFC ( $t = 10.53, p = .0002$  FWE-corrected), the DLPFC and anterior insula ( $t = 4.34, p = .0006$  FWE-corrected), and the VMPFC and DLPFC ( $t = 6.78, p = .0002$  FWE-corrected). There was also a trend toward positive connectivity between the anterior insula and amygdala, which did not survive correction for multiple comparisons, ( $t = 2.37, p$  uncorrected =  $.013, p = .065$  FWE-corrected). Group-level negative connectivity was found between the VMPFC and the anterior

**Figure 1.** Results of a group-level *t* test performed on partial connectivity matrices. Partial connectivity matrices were calculated separately for “safe” and “shock anticipation” scans and averaged within each individual before performing a Student’s *t* test. Colors indicate *t* statistics. Connections that reach significance after FWE correction ( $p < .05$  corrected) are marked with asterisks.



insula ( $t = -5.55, p = .0002$  FWE-corrected). There was no significant direct connectivity between DLPFC and amygdala ( $t = -1.63, p = .24$  FWE-corrected).

### Changes in Group-level Connectivity during Shock Receipt and Shock Anticipation versus Safe

A two-tailed paired  $t$  test was performed to compare the connectivity matrices during the 15 min of “shock anticipation” to the “safe” scan to determine group-level changes in connectivity related to anticipation of shock, across all participants regardless of anxiety levels. There were trends for the following regions to show increased connectivity under threat of shock: amygdala–anterior insula ( $t = 1.83$ , uncorrected  $p = .036$ ), DLPFC–anterior insula ( $t = 1.73$ , uncorrected  $p = .05$ ), and VMPFC–amygdala ( $t = 1.59$ , uncorrected  $p = .058$ ), but none of these results survived after correction for multiple comparisons ( $p > .2$  FWE-corrected). Given our prediction that these connections might vary as a function of trait anxious affect or induced anxiety, it was not unexpected that only weak effects were seen at the group level.

We next compared the “initial shock” period (first 5 min) of the second scan, during which 15 discrete electrical shocks were administered at varied intervals, to the first 5 min of the “safe” scan, during which no electric shocks were administered, to investigate changes in connectivity in the period that contained intermittent receipt of shocks. Results revealed a significant increase in connectivity between the anterior insula and the DLPFC ( $p = .048$  FWE-corrected) during this “initial shock” period. There was also a trend for an increase in amygdala–anterior insula connectivity, but this did not reach significance after correction for multiple comparisons ( $p = .023$  uncorrected;  $p = .13$  FWE-corrected).

### Anxious Affect Linked to Reduced Change in VMPFC–Amygdala Connectivity between Safe and Anticipation of Shock Periods

Scores on the latent dimension of anxious affect were inversely associated with increases in VMPFC–amygdala connectivity during anticipation of shock, relative to during the “safe” scan ( $t = 2.55, r = -.42, p = .045$  FWE-corrected; Figure 2A). Figure 2B shows that participants with a below mean score on this latent dimension showed an increase in connectivity between the amygdala and the VMPFC during anticipation of shock versus safety, whereas participants with an above mean score showed little change in connectivity between these periods. These findings held when induced anxiety scores were entered in the model as a control covariate ( $t = 2.49, r = -.42, p = .051$  FWE-corrected). There were no other regions for which changes in connectivity from “safe” to “anticipation of shock” varied significantly as a function of trait anxious affect,  $ps > .1$ , uncorrected.

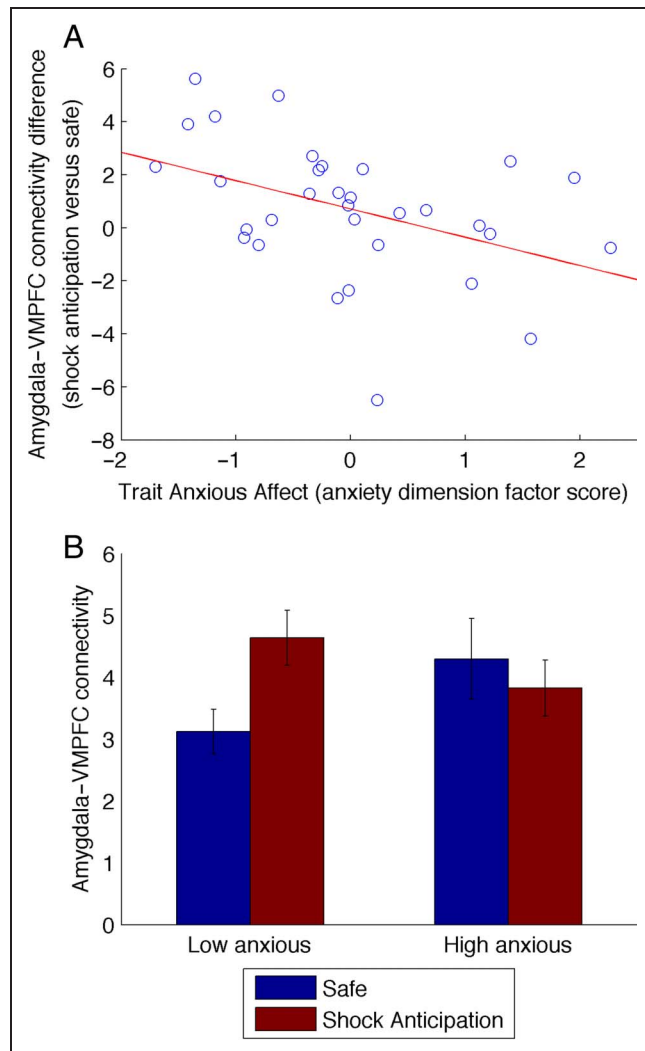


**Figure 2.** Relationship between participant trait anxious affect and amygdala–VMPFC connectivity during “shock anticipation” versus “safe” scans. (A) There was a significant negative correlation between trait anxious affect (i.e., scores on the anxiety-related latent dimension obtained from scores on the mood and personality questionnaires administered) and change in amygdala–VMPFC connectivity (“shock anticipation” minus “safe”). (B) For illustrative purposes, a mean split was conducted on trait anxious affect. The plot here shows amygdala–VMPFC connectivity strength separately for “safe” and “shock anticipation” scans for “low anxious” ( $n = 19$ ) and “high anxious” ( $n = 13$ ) participants. Error bars indicate SEM.

To further explore the finding reported here, we investigated the correlation between anxious affect and VMPFC–amygdala connectivity separately for the “safe” and “shock anticipation” periods. These analyses revealed a positive correlation between amygdala–VMPFC connectivity and anxious affect during the “safe” scan ( $t = 1.77, r = .31, p = .042$ ). Conversely, during “shock anticipation,” there was a trend-level negative correlation between VMPFC–amygdala connectivity and anxious affect ( $t = -1.42, r = -.25, p = .077$ ). These results show that the direction of the correlation between VMPFC–amygdala connectivity and the anxiety-related latent dimension reversed as a

function of the shock manipulation. Specifically, participants with above mean scores on the anxious affect dimension ( $n = 13$ ) showed stronger VMPFC–amygdala connectivity during the “safe” scan but failed to increase connectivity during anticipation of shocks. Individuals with below mean scores on the anxious affect dimension ( $n = 19$ ), on the other hand, showed an increase in VMPFC–amygdala connectivity from the “safe” to the “shock anticipation” period.

To further illustrate the temporal dynamics underlying this result, we calculated partial connectivity for non-overlapping 2.5-min time windows during the “safe” scan, the 5-min shock period at the start of the second scan (“initial shock”), and the “shock anticipation” period from the second scan. Figure 3 uses these data to illustrate the findings presented above at a finer temporal scale. To determine whether changes in VMPFC–amygdala connectivity were sustained throughout the 15-min “shock anticipation” period versus waning or increasing across

this period, we fitted a straight line to each participant’s VMPFC–amygdala connectivity strength measured across the six 2.5-min time windows from this period. Results revealed that no significant linear slope was found (mean slope = 0, one-group  $t$  test  $p = .39$ ). Neither the slope nor the residuals of the linear fit were correlated with the latent dimension of anxiety or with induced anxiety ( $ps > .1$ ).

### Induced Anxiety Linked to Reduced Augmentation of DLPFC–Anterior Insula Connectivity during Anticipation of Shock

Participants varied in the extent to which they showed an increase in anxiety as a result of the shock manipulation (induced anxiety as measured by change in visual analogue ratings). Across participants, extent of induced anxiety was significantly negatively correlated with change in DLPFC–anterior insula connectivity during anticipation of

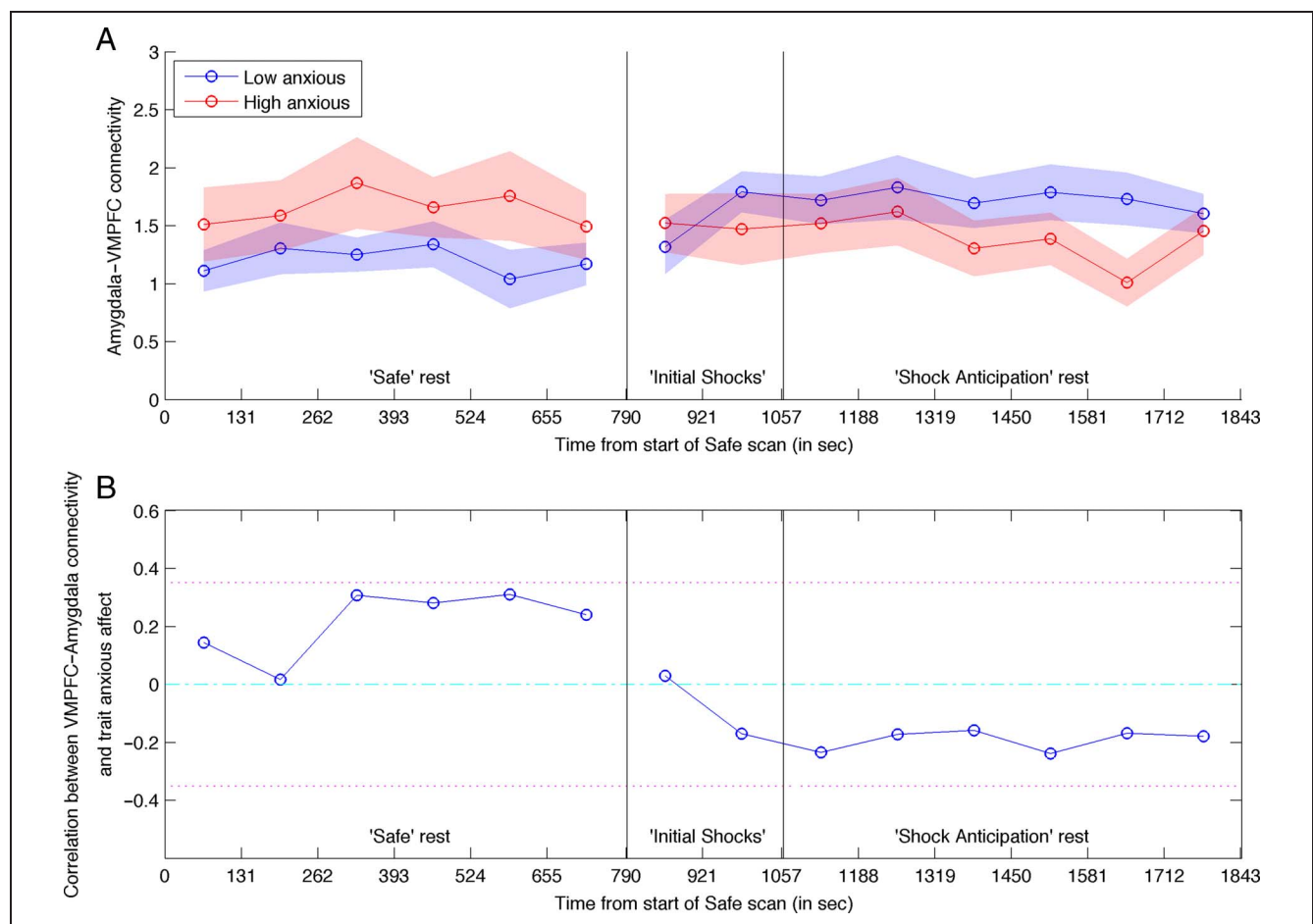


**Figure 3.** Changes in dynamic connectivity between the amygdala and VMPFC as measured using 2.5-min shifting windows. (A) Z-transformed partial connectivity between the amygdala and VMPFC was estimated separately for each time window. This is plotted separately for high and low anxious participants (i.e., those with above vs. below mean trait anxious affect; see Figure 2 and Methods section). Line bounds indicate SEM across participants within each group. (B) Pearson’s correlation between windowed amygdala–VMPFC connectivity and trait anxious affect. Dotted magenta lines indicate two-tailed uncorrected significance level for  $n = 32$ . The vertical line-break signifies the break between the “safe” and “shock” scans. This figure is included for illustration purposes to represent the stationary findings presented in Figure 2 at a finer temporal scale.

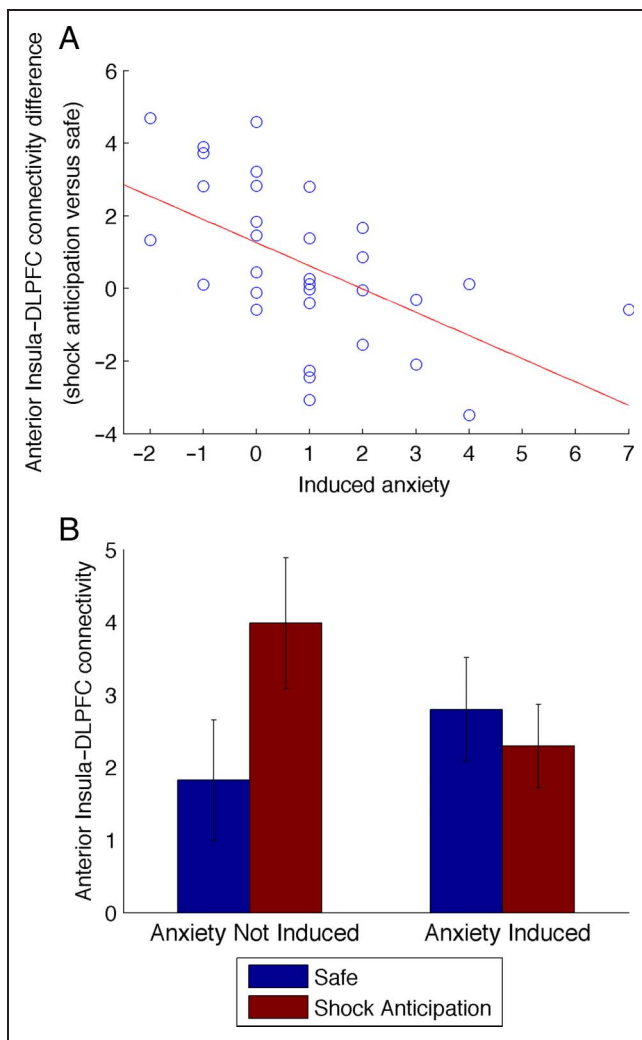


**Figure 4.** Induced anxiety is linked to reduced anterior insula-DLPFC connectivity during “shock anticipation.” (A) There was a significant negative correlation between the change in anterior insula-DLPFC connectivity (“shock anticipation” minus “safe”) and induced anxiety scores (i.e., the difference in anxiety experienced during the shock vs. the safe scan, as assessed immediately following each scan using a visual analogue scale from 1 to 7). (B) For illustrative purposes, participants were split into two groups: “Anxiety Not Induced” (induced anxiety score  $\leq 0$ ;  $n = 14$ ) and “Anxiety Induced” (induced anxiety score  $> 0$ ;  $n = 18$ ). Anterior insula-DLPFC connectivity is shown separately for “safe” and “shock anticipation” periods. Error bars indicate *SEM*.

shock versus during the “safe” scan ( $t = 3.61$ ,  $r = -.55$ ,  $p = .004$  FWE-corrected; Figure 4A). This result remained significant when participants’ score on the latent dimension of anxiety-related affect was entered in the model as a covariate of no interest ( $t = 3.61$ ,  $r = -.56$ ,  $p = .004$  FWE-corrected). Figure 4B shows that participants who reported no induced anxiety as a result of the shock manipulation showed an increase in DLPFC–anterior insula connectivity during shock anticipation relative to during the “safe” scan. Participants who reported induction of anxiety by the shock manipulation did not show such a change in connectivity. There were no other

regions for which changes in connectivity from “safe” to “anticipation of shock” varied significantly as a function of induced anxiety,  $ps > .1$ , uncorrected.

As for the VMPFC–amygdala connectivity analyses described above, we next performed separate regression analyses for connectivity during the “safe” and “shock anticipation” periods, respectively. Findings revealed that there was no significant relationship between DLPFC–anterior insula connectivity and induced anxiety during the “safe” scan ( $r = .08$ ,  $p > .6$ ). During “shock anticipation,” there was a significant negative relationship between DLPFC–anterior insula connectivity and induced anxiety ( $t = -1.85$ ,  $r = -.32$ ,  $p = .038$ ). In other words, the relationship between DLPFC–anterior insula connectivity and induced anxiety was driven by individual differences in connectivity during the “shock anticipation” period.

To further examine the temporal dynamics of DLPFC–anterior insula connectivity, we calculated partial correlations for nonoverlapping 2.5-min windows across the “safe,” “initial shock,” and “shock anticipation” periods. Results are shown in Figure 5 and illustrate the findings reported above at a finer temporal scale. Application of a linear fit to data from the six 2.5-min windows during “shock anticipation” enabled us to establish if DLPFC–anterior insula connectivity increased or decreased significantly across the anticipation period. The slope of this function was not significantly different from zero (mean slope = 0, one-group  $t$  test  $p = .26$ ). Furthermore, neither the slope nor the residuals were significantly correlated with induced anxiety or with the latent anxiety-related dimension ( $ps > .1$ ).

## Replication of Amygdala–aMCC Results

Given the value of replication across studies, we additionally investigated functional connectivity between the amygdala and the aMCC, given the recent findings by Vytal and colleagues of increased connectivity between these regions, especially in high trait anxious individuals, during prolonged anticipation of shock (Vytal et al., 2014). During the “shock anticipation” period, amygdala–aMCC connectivity strength was significantly positively associated with our latent dimension of anxious affect ( $t = 1.82$ ,  $p = .038$ ; Figure 6). These findings support and extend those reported by Vytal et al. (2014), given our use of partial correlation to calculate direct functional connectivity.

## DISCUSSION

Our results reveal dissociable correlates of individual differences in trait anxious affect versus induced anxiety with functional connectivity under prolonged anticipation of shock. Trait anxious affect was negatively associated with the extent of VMPFC–amygdala connectivity

during anticipation of shock relative to the baseline “safe” scan. Meanwhile, induced anxiety was inversely correlated with DLPFC–anterior insula connectivity during anticipation of shock versus safety. Specifically, those participants who showed an increase in DLPFC–anterior insula connectivity during anticipation of shock relative to the “safe” scan, reported lower levels of induced anxiety as a result of the shock manipulation. We also replicated prior findings of a positive relationship between trait anxious affect and amygdala–aMCC connectivity during prolonged anticipation of shock (Vytal et al., 2014).

Both human and basic neuroscience studies have pointed to a role for VMPFC in the regulation and extinction of fear and anxiety responses (Indovina, Robbins, Núñez-Elizalde, Dunn, & Bishop, 2011; Milad et al., 2007; Phelps, Delgado, Nearing, & LeDoux, 2004). It has been argued that, in humans, this phylogenetically old circuitry may support automatic emotion regulation more broadly

(Silvers, Wager, Weber, & Ochsner, 2014; Mauss et al., 2007). The current finding that individuals with low, but not high, anxious affect showed an increase in VMPFC–amygdala connectivity during anticipation of shock is in line with the suggestion that connectivity between these regions may support regulation of emotional responses. The ability to flexibly engage this circuitry may support emotional resilience, with those less able to recruit this circuitry under conditions of prolonged threat potentially being more susceptible to pathological anxiety.

Interestingly, further exploration of the data revealed that, although there was no relationship between trait anxious affect and levels of anxiety participants reported experiencing during the “safe” scan, individuals scoring high in anxious affect showed elevated VMPFC–amygdala connectivity during the “safe” scan, compared with low scoring participants (Figure 3). Participants with low anxious affect showed a much greater increase in connectivity during shock anticipation, which led to a reversal

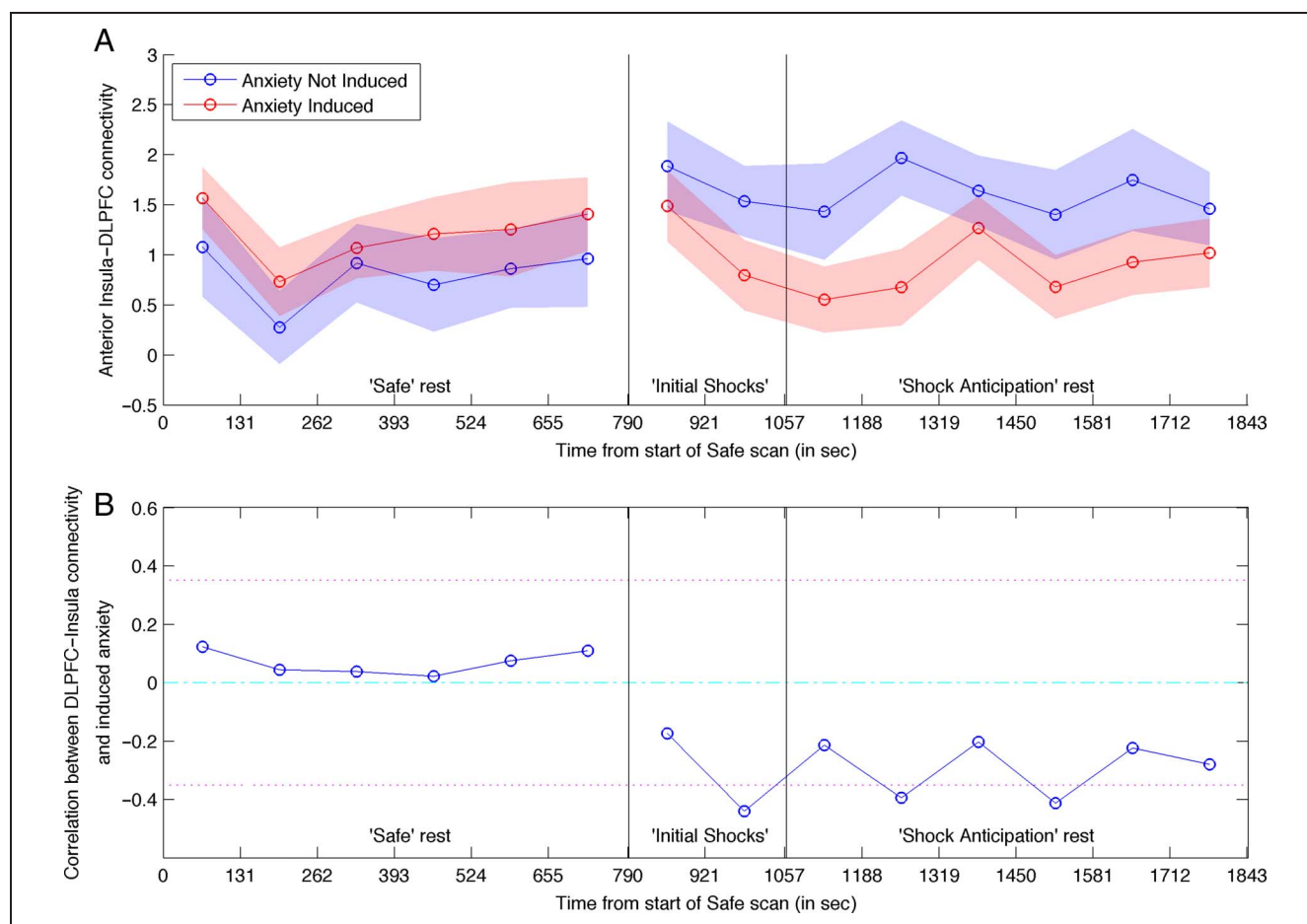


**Figure 5.** Changes in dynamic connectivity between the anterior insula and DLPFC as measured using 2.5-min shifting windows. (A) Z-transformed partial connectivity between the anterior insula and DLPFC for each time window as a function of whether participants experienced induced anxiety as a result of the shock manipulation (groups: Anxiety Induced, Anxiety Not Induced). Line bounds indicate *SEM* across participants within each group. (B) Pearson’s correlation coefficients between windowed anterior insula–DLPFC connectivity and induced anxiety (continuous difference score for anxiety experienced during shock scan minus anxiety experienced during safe scan). Dotted magenta lines indicate two-tailed uncorrected significance level for  $n = 32$ . The vertical line-break signifies the break between the “safe” and “shock” scans. This figure is included for illustration purposes to represent the stationary findings presented in Figure 4 at a finer temporal scale.

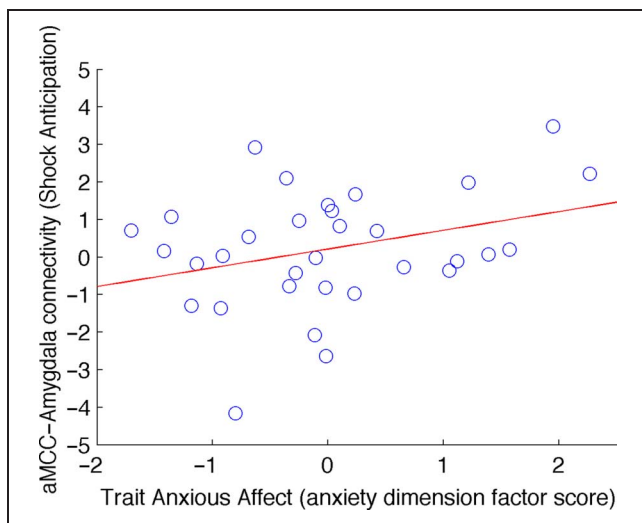


**Figure 6.** Targeted analyses of amygdala–aMCC connectivity aimed to determine if we would replicate findings by Vytal et al. (2014). As reported by Vytal et al. (2014), we observed a significant positive correlation between amygdala–aMCC connectivity during “shock anticipation” and trait anxious affect (here as assessed by factor scores on our anxiety-related latent dimension).

of the relationship between anxious affect and VMPFC–amygdala connectivity during anticipation of shock. One possible interpretation is that high trait anxious affect individuals were engaged in maximal levels of automatic regulation during the “safe” scans, potentially reflecting the mildly stressful experience of the MRI scanner and the knowledge that shock would be experienced in future scans, and were unable to further increase engagement of this circuitry during the “anticipation of shock” period. Under anticipation of shock, participants low in trait anxious affect surpassed the level of VMPFC–amygdala connectivity shown by individuals high in trait anxious affect, indicating greater flexibility to bring this circuitry robustly online in a context appropriate manner.

We turn next to the relationship, across participants, between DLPFC–anterior insula connectivity during anticipation of shock and individual differences in anxiety induced by the shock manipulation. DLPFC has been suggested to play a role in reappraisal and the deliberate regulation of emotional responses (Hartley & Phelps, 2010). Meanwhile, findings that anterior insula activation during anticipation of threat is enhanced in anxiety-prone individuals and those with anxiety disorders, shows a positive correlation with self-reported induced anxiety, and is negatively associated with trait differences in use of reappraisal have led to the suggestion that the anterior insula may be involved in the experience of anticipatory anxiety as opposed to its regulation and might further potentially be a target for regulatory influences (Carlson et al., 2011; Carlson & Mujica-Parodi, 2010; Straube et al., 2007; Simmons et al., 2006). Prior work from our group has revealed that, at rest, trait anxious affect is linked to

reduced functional connectivity between the anterior insula and both other frontal regions and the amygdala (Bijsterbosch et al., 2013). These findings can be reconciled by models proposing that the insula acts as a “hub” region, enabling bidirectional information flow between frontal control regions such as the DLPFC and subcortical regions (Menon & Uddin, 2010). In the context of such models, increased connectivity between DLPFC and anterior insula might reflect top–down regulatory signaling from DLPFC to the anterior insula, aimed at diminishing anticipatory anxiety responses. Our current findings indicated that increased DLPFC–anterior insula connectivity during anticipation of shock was negatively associated with induced anxiety. This result fits well with the notion that individuals with a disposition to engage in reappraisal without instruction may bring this circuitry online to successfully reduce subjective levels of anticipatory anxiety. In future work, it will be interesting to administer measures of trait disposition to engage in reappraisal to see if this is indeed the case. Intriguingly, there was no significant relationship between DLPFC–anterior insula connectivity and participant trait anxious affect and only a weak trend toward a positive relationship between participant trait anxious affect and anxiety induced by the shock manipulation. One possible interpretation of this is that this DLPFC–anterior insula pathway might provide an alternate route to the phylogenetically earlier VMPFC–amygdala circuitry for achieving down-regulation of anticipatory anxiety when a stressor is anticipated and that this might mitigate the effects of impoverished VMPFC–amygdala recruitment in some individuals with high trait anxious affect.

Finally, we replicated the finding that trait anxious affect is positively associated with aMCC–amygdala connectivity during shock anticipation (Vytal et al., 2014). The aMCC has been implicated in the processing of pain, emotional stimuli, and otherwise salient or surprising stimuli (Hayden, Heilbronner, Pearson, & Platt, 2011; Shackman et al., 2011; Seeley et al., 2007). It has further been argued to provide a route by which information on the need to reassign processing priorities can be passed forward to frontal control regions (Botvinick, Cohen, & Carter, 2004). As such, the aMCC has also been proposed to be an important “hub” or “connector node” in network terms (Grube & Nitschke, 2013; Shackman et al., 2011). Increased aMCC–amygdala signaling during anticipation of threat in individuals with high trait anxious affect might reflect the ongoing experience of anticipatory anxiety and vigilance to threat in the absence of successful engagement of regulatory mechanisms, in particular the down-regulation of amygdala activity by VMPFC. Our replication of this finding provides support for the robustness of this relationship. We hope that future studies will likewise seek to establish the replicability of the other findings reported here.

In summary, our findings indicate that individual differences in functional integrity of networks supporting emotion regulation may be linked to resilience against, versus

vulnerability to, anxiety. Our results support the suggestion that there may be two distinct emotion regulation circuits, one involving the VMPFC and the amygdala, and the other the DLPFC and the anterior insula. Our findings indicate that the recruitment of these networks is differentially related to low levels of trait anxious affect versus the ability to down-regulate anxiety induced by the situation or context. Our findings further suggest that individuals with low trait anxious affect are differentiated from those with high anxious affect by the flexible engagement of VMPFC–amygdala circuitry under conditions of elevated expectation of threat. Specifically, our findings suggest that individuals with high trait anxious affect potentially use this mechanism relatively inefficiently (Eysenck, Derakshan, Santos, & Calvo, 2007), having it in “full throttle” even under relatively low stress contexts. Our findings also point to the presence of an alternate DLPFC–anterior insula regulatory pathway linked to individual differences in the ability to minimize induced anxiety as opposed to more long-standing trait anxious affect. The findings of individual differences in VMPFC–amygdala and DLPFC–anterior insula connectivity that are largely independent of each other and related to different aspects of the experience of anxiety suggest that these two networks might well provide valuable complementary targets for future intervention-oriented research.

## Acknowledgments

This research was supported by grants from the National Institute of Mental Health (R01MH091848) and the European Research Community (GA 260932). The authors acknowledge the receipt of the Pulse Sequence and Reconstruction Algorithms from the Center for Magnetic Resonance Research, University of Minnesota.

Reprint requests should be sent to Janine Bijsterbosch, FMRIB Centre, Nuffield Department of Clinical Neurosciences, John Radcliffe Hospital, University of Oxford, Oxford, OX3 0LY, UK, or via e-mail: Janine.Bijsterbosch@ndcn.ox.ac.uk or Sonia J. Bishop, Department of Psychology, University of California, Berkeley, 5315 Tolman Hall, Berkeley, CA 94720-1650, or via e-mail: sbishop@berkeley.edu.

## REFERENCES

- Andersson, J. L. R., Jenkinson, M., & Smith, S. M. (2007a). *Non-linear optimisation. FMRIB Technical Report* (Vol. 7). <http://www.fmrib.ox.ac.uk/analysis/techrep/tr07ja1.pdf>.
- Andersson, J. L. R., Jenkinson, M., & Smith, S. M. (2007b). *Non-linear registration, aka spatial normalisation. FMRIB Technical Report* (Vol. 7). <http://www.fmrib.ox.ac.uk/analysis/techrep/tr07ja2/tr07ja2.pdf>.
- Beck, A. T., Ward, C. H., Mendelson, M., Mock, J., & Erbaugh, J. (1961). An inventory for measuring depression. *Archives of General Psychiatry*, *4*, 561–571.
- Beckmann, C. F., & Smith, S. M. (2004). Probabilistic independent component analysis for functional magnetic resonance imaging. *IEEE Transactions on Medical Imaging*, *23*, 137–152.
- Bieling, P. J., Antony, M. M., & Swinson, R. P. (1998). The State-Trait Anxiety Inventory, Trait version: Structure and content re-examined. *Behaviour Research and Therapy*, *36*, 777–788.
- Bijsterbosch, J. D., Smith, S. M., Forster, S., John, O. P., & Bishop, S. J. (2013). Resting state correlates of subdimensions of anxious affect. *Journal of Cognitive Neuroscience*, *4*, 1–13.
- Bishop, S. J. (2007). Neurocognitive mechanisms of anxiety: An integrative account. *Trends in Cognitive Sciences*, *11*, 307–316.
- Botvinick, M. M., Cohen, J. D., & Carter, C. S. (2004). Conflict monitoring and anterior cingulate cortex: An update. *Trends in Cognitive Sciences*, *8*, 539–546.
- Buhle, J. T., Silvers, J. A., Wager, T. D., Lopez, R., Onyemkwe, C., Kober, H., et al. (2014). Cognitive reappraisal of emotion: A meta-analysis of human neuroimaging studies. *Cerebral Cortex*, *24*, 2981–2990.
- Carlson, J. M., Greenberg, T., Rubin, D., & Mujica-Parodi, L. R. (2011). Feeling anxious: Anticipatory amygdalo-insular response predicts the feeling of anxious anticipation. *Social Cognitive and Affective Neuroscience*, *6*, 74–81.
- Carlson, J. M., & Mujica-Parodi, L. R. (2010). A disposition to reappraise decreases anterior insula reactivity during anxious anticipation. *Biological Psychology*, *85*, 383–385.
- Cusack, R., Brett, M., & Osswald, K. (2003). An evaluation of the use of magnetic field maps to undistort echo-planar images. *Neuroimage*, *18*, 127–142.
- Davis, M., Walker, D. L., Miles, L., & Grillon, C. (2010). Phasic vs. sustained fear in rats and humans: Role of the extended amygdala in fear vs anxiety. *Neuropsychopharmacology*, *35*, 105–135.
- Delgado, M. R., Olsson, A., & Phelps, E. A. (2006). Extending animal models of fear conditioning to humans. *Biological Psychology*, *73*, 39–48.
- Eysenck, H. J., & Eysenck, S. B. G. (1975). *Eysenck Personality Questionnaire manual*. San Diego, CA: Educational and Industrial Testing Service.
- Eysenck, M. W., Derakshan, N., Santos, R., & Calvo, M. G. (2007). Anxiety and cognitive performance: Attentional control theory. *Emotion*, *7*, 336–353.
- Feinberg, D. A., Moeller, S., Smith, S. M., Auerbach, E. J., Ramanna, S., Glasser, M. F., et al. (2010). Multiplexed echo planar imaging for sub-second whole brain fMRI and fast diffusion imaging. *PLoS ONE*, *5*, e15710.
- Fox, A. S., Shelton, S. E., Oakes, T. R., Davidson, R. J., & Kalin, N. H. (2008). Trait-like brain activity during adolescence predicts anxious temperament in primates. *PLoS One*, *3*, e2570.
- Glasser, M. F., Sotiropoulos, S. N., Wilson, J. A., Coalson, T. S., Fischl, B., Andersson, J. L. R., et al. (2013). The minimal preprocessing pipelines for the Human Connectome Project. *Neuroimage*, *80*, 105–124.
- Goossens, K. A. (2001). Contextual and auditory fear conditioning are mediated by the lateral, basal, and central amygdaloid nuclei in rats. *Learning & Memory*, *8*, 148–155.
- Greve, D. N., & Fischl, B. (2009). Accurate and robust brain image alignment using boundary-based registration. *Neuroimage*, *48*, 63–72.
- Griffanti, L., Salimi-Khorshidi, G., Beckmann, C. F., Auerbach, E. J., Douaud, G., Sexton, C. E., et al. (2014). ICA-based artefact removal and accelerated fMRI acquisition for improved resting state network imaging. *Neuroimage*, *95*, 232–247.
- Grillon, C. (2002). Startle reactivity and anxiety disorders: Aversive conditioning, context, and neurobiology. *Biological Psychiatry*, *52*, 958–975.
- Grupe, D. W., & Nitschke, J. B. (2013). Uncertainty and anticipation in anxiety: An integrated neurobiological and

- psychological perspective. *Nature Reviews Neuroscience*, *14*, 488–501.
- Grupe, D. W., Oathes, D. J., & Nitschke, J. B. (2013). Dissecting the anticipation of aversion reveals dissociable neural networks. *Cerebral Cortex*, *23*, 1874–1883.
- Hartley, C. A., & Phelps, E. A. (2010). Changing fear: The neurocircuitry of emotion regulation. *Neuropsychopharmacology*, *35*, 136–146.
- Hayden, B. Y., Heilbronner, S. R., Pearson, J. M., & Platt, M. L. (2011). Surprise signals in anterior cingulate cortex: Neuronal encoding of unsigned reward prediction errors driving adjustment in behavior. *Journal of Neuroscience*, *31*, 4178–4187.
- Indovina, I., Robbins, T. W., Núñez-Elizalde, A. O., Dunn, B. D., & Bishop, S. J. (2011). Fear-conditioning mechanisms associated with trait vulnerability to anxiety in humans. *Neuron*, *69*, 563–571.
- Jenkinson, M., Bannister, P., Brady, M., & Smith, S. M. (2002). Improved optimization for the robust and accurate linear registration and motion correction of brain images. *Neuroimage*, *17*, 825–841.
- Jenkinson, M., & Smith, S. M. (2001). A global optimisation method for robust affine registration of brain images. *Medical Image Analysis*, *5*, 143–156.
- Jezzard, P., & Balaban, R. S. (1995). Correction for geometric distortion in echo planar images from B0 field variations. *Magnetic Resonance in Medicine*, *34*, 65–73.
- Kalin, N. H. (2004). The role of the central nucleus of the amygdala in mediating fear and anxiety in the primate. *Journal of Neuroscience*, *24*, 5506–5515.
- Kalisch, R., Wiech, K., Critchley, H. D., Seymour, B., O'Doherty, J. P., Oakley, D. A., et al. (2005). Anxiety reduction through detachment: Subjective, physiological, and neural effects. *Journal of Cognitive Neuroscience*, *17*, 874–883.
- Kim, M. J., Gee, D. G., Loucks, R. A., Davis, F. C., & Whalen, P. J. (2011). Anxiety dissociates dorsal and ventral medial prefrontal cortex functional connectivity with the amygdala at rest. *Cerebral Cortex*, *21*, 1667–1673.
- Kim, M. J., & Whalen, P. J. (2009). The structural integrity of an amygdala-prefrontal pathway predicts trait anxiety. *Journal of Neuroscience*, *29*, 11614–11618.
- Kochli, D. E., Thompson, E. C., Fricke, E. A., Postle, A. F., & Quinn, J. J. (2015). The amygdala is critical for trace, delay, and contextual fear conditioning. *Learning & Memory*, *22*, 92–100.
- LeDoux, J. (2003). The emotional brain, fear, and the amygdala. *Cellular and Molecular Neurobiology*, *23*, 727–738.
- Maren, S., Phan, K. L., & Liberzon, I. (2013). The contextual brain: Implications for fear conditioning, extinction and psychopathology. *Nature Reviews Neuroscience*, *14*, 417–428.
- Marrelec, G., Krainik, A., Duffau, H., Péligrini-Issac, M., Lehéricy, S., Doyon, J., et al. (2006). Partial correlation for functional brain interactivity investigation in functional MRI. *Neuroimage*, *32*, 228–237.
- Mauss, I. B., Bunge, S. A., & Gross, J. J. (2007). Automatic emotion regulation. *Social and Personality Psychology Compass*, *1*, 146–167.
- McMenamin, B. W., Langeslag, S. J. E., Sirbu, M., Padmala, S., & Pessoa, L. (2014). Network organization unfolds over time during periods of anxious anticipation. *Journal of Neuroscience*, *34*, 11261–11273.
- Menon, V., & Uddin, L. Q. (2010). Saliency, switching, attention and control: A network model of insula function. *Brain Structure and Function*, *214*, 655–667.
- Meyer, T. J., Miller, M. L., Metzger, R. L., & Borkovec, T. D. (1990). Development and validation of the Penn State Worry Questionnaire. *Behaviour Research and Therapy*, *28*, 487–495.
- Milad, M. R., & Quirk, G. J. (2002). Neurons in medial prefrontal cortex signal memory for fear extinction. *Nature*, *420*, 70–74.
- Milad, M. R., & Quirk, G. J. (2012). Fear extinction as a model for translational neuroscience: Ten years of progress. *Annual Review of Psychology*, *63*, 129–151.
- Milad, M. R., Wright, C. I., Orr, S. P., Pitman, R. K., Quirk, G. J., & Rauch, S. L. (2007). Recall of fear extinction in humans activates the ventromedial prefrontal cortex and hippocampus in concert. *Biological Psychiatry*, *62*, 446–454.
- Moeller, S., Yacoub, E. S., Oelman, C. A., Auerbach, E. J., Strupp, J., Harel, N., et al. (2010). Multiband multislice GE-EPI at 7 tesla, with 16-fold acceleration using partial parallel imaging with application to high spatial and temporal whole-brain fMRI. *Magnetic Resonance in Medicine*, *63*, 1144–1153.
- Motzkin, J. C., Philippi, C. L., Wolf, R. C., Baskaya, M. K., & Koenigs, M. (2015). Ventromedial prefrontal cortex is critical for the regulation of amygdala activity in humans. *Biological Psychiatry*, *77*, 276–284.
- Nitschke, J. B., Sarinopoulos, I., Mackiewicz, K. L., Schaefer, H. S., & Davidson, R. J. (2006). Functional neuroanatomy of aversion and its anticipation. *Neuroimage*, *29*, 106–116.
- Nitschke, J. B., Sarinopoulos, I., Oathes, D. J., Johnstone, T., Whalen, P. J., Davidson, R. J., et al. (2009). Anticipatory activation in the amygdala and anterior cingulate in generalized anxiety disorder and prediction of treatment response. *American Journal of Psychiatry*, *166*, 302–310.
- Onishi, B. K. A., & Xavier, G. F. (2010). Contextual, but not auditory, fear conditioning is disrupted by neurotoxic selective lesion of the basal nucleus of amygdala in rats. *Neurobiology of Learning and Memory*, *93*, 165–174.
- Phelps, E. A., Delgado, M. R., Nearing, K. I., & LeDoux, J. E. (2004). Extinction learning in humans: Role of the amygdala and vmPFC. *Neuron*, *43*, 897–905.
- Ploghaus, A., Tracey, I., Gati, J. S., Clare, S., Menon, R. S., Matthews, P. M., et al. (1999). Dissociating pain from its anticipation in the human brain. *Science*, *284*, 1979–1981.
- Radloff, L. S. (1977). The CES-D Scale: A self-report depression scale for research in the general population. *Applied Psychological Measurement*, *1*, 385–401.
- Salimi-Khorshidi, G., Douaud, G., Beckmann, C. F., Glasser, M. F., Griffanti, L., & Smith, S. M. (2014). Automatic denoising of functional MRI data: Combining independent component analysis and hierarchical fusion of classifiers. *Neuroimage*, *90*, 449–468.
- Seeley, W. W., Menon, V., Schatzberg, A. F., Keller, J., Glover, G. H., Kenna, H., et al. (2007). Dissociable intrinsic connectivity networks for salience processing and executive control. *Journal of Neuroscience*, *27*, 2349–2356.
- Shackman, A. J., Salomons, T. V., Slagter, H. A., Fox, A. S., Winter, J. J., & Davidson, R. J. (2011). The integration of negative affect, pain and cognitive control in the cingulate cortex. *Nature Reviews Neuroscience*, *12*, 154–167.
- Sierra-Mercado, D., Padilla-Coreano, N., & Quirk, G. J. (2011). Dissociable roles of prelimbic and infralimbic cortices, ventral hippocampus, and basolateral amygdala in the expression and extinction of conditioned fear. *Neuropsychopharmacology*, *36*, 529–538.
- Silvers, J. A., Wager, T. D., Weber, J., & Ochsner, K. N. (2014). The neural bases of uninstructed negative emotion modulation. *Social Cognitive and Affective Neuroscience*, *10*, 10–18.
- Simmons, A. N., Strigo, I. A., Matthews, S. C., Paulus, M. P., & Stein, M. B. (2006). Anticipation of aversive visual stimuli is associated with increased insula activation in anxiety-prone subjects. *Biological Psychiatry*, *60*, 402–409.
- Smith, S. M. (2002). Fast robust automated brain extraction. *Human Brain Mapping*, *17*, 143–155.

- Smith, S. M., Beckmann, C. F., Andersson, J. L. R., Auerbach, E. J., Bijsterbosch, J. D., Douaud, G., et al. (2013). Resting-state fMRI in the Human Connectome Project. *Neuroimage*, *80*, 144–168.
- Somerville, L. H., Wagner, D. D., Wig, G. S., Moran, J. M., Whalen, P. J., & Kelley, W. M. (2013). Interactions between transient and sustained neural signals support the generation and regulation of anxious emotion. *Cerebral Cortex*, *23*, 49–60.
- Sotres-Bayon, F., Bush, D. E. A., & LeDoux, J. E. (2004). Emotional perseveration: An update on prefrontal-amygdala interactions in fear extinction. *Learning & Memory*, *11*, 525–535.
- Sotres-Bayon, F., Sierra-Mercado, D., Pardilla-Delgado, E., & Quirk, G. J. (2012). Gating of fear in prelimbic cortex by hippocampal and amygdala inputs. *Neuron*, *76*, 804–812.
- Spielberger, C. D. (1983). *Manual for the State-Trait Anxiety Inventory*. Palo Alto, CA: Consulting Psychologists Press.
- Straube, T., Mentzel, H.-J., & Miltner, W. H. R. (2007). Waiting for spiders: Brain activation during anticipatory anxiety in spider phobics. *Neuroimage*, *37*, 1427–1436.
- Ugurbil, K., Xu, J., Auerbach, E. J., Moeller, S., Vu, A. T., Duarte-Carvajalino, J. M., et al. (2013). Pushing spatial and temporal resolution for functional and diffusion MRI in the Human Connectome Project. *Neuroimage*, *80*, 80–104.
- Vytal, K. E., Overstreet, C., Charney, D. R., Robinson, O. J., & Grillon, C. (2014). Sustained anxiety increases amygdala-dorsomedial prefrontal coupling: A mechanism for maintaining an anxious state in healthy adults. *Journal of Psychiatry & Neuroscience*, *39*, 130145.
- Watson, D., & Clark, L. A. (1991). *The Mood and Anxiety Symptom Questionnaire*. Iowa City, IA: University of Iowa.
- Watson, D., Weber, K., Assenheimer, J. S., Clark, L. A., Strauss, M. E., & McCormick, R. A. (1995). Testing a tripartite model: I. Evaluating the convergent and discriminant validity of anxiety and depression symptom scales. *Journal of Abnormal Psychology*, *104*, 3–14.